

## Bond-length relaxation in crystalline $\text{Si}_{1-x}\text{Ge}_x$ alloys: An extended x-ray-absorption fine-structure study

Hiroshi Kajiyama

*Advanced Research Laboratory, Hitachi, Ltd., Saitama 350-03, Japan*

Shin-ichi Muramatsu and Toshikazu Shimada

*Central Research Laboratory, Hitachi, Ltd., Tokyo 185, Japan*

Yoichi Nishino

*Department of Materials Science and Engineering, Nagoya Institute of Technology, Nagoya 466, Japan*

(Received 21 January 1992)

Extended x-ray-absorption fine-structure spectra for crystalline  $\text{Si}_{1-x}\text{Ge}_x$  alloys, measured at the  $K$  edge of Ge at room temperature, are analyzed with a curve-fitting method based on the spherical-wave approximation. The Ge-Ge and Ge-Si bond lengths, coordination numbers of Ge and Si atoms around a Ge atom, and Debye-Waller factors of Ge and Si atoms are obtained. It is shown that Ge-Ge and Ge-Si bonds relax completely, for all Ge concentrations of their study, while the lattice constant varies monotonically, following Vegard's law. As noted by Bragg and later by Pauling and Huggins, the Ge-Ge and Ge-Si bond lengths are close to the sum of their constituent-element atomic radii: nearly 2.45 Å for Ge-Ge bonds and 2.40 Å for Ge-Si bonds. A study on the coordination around a Ge atom in the alloys revealed that Ge and Si atoms mix randomly throughout the compositional range studied.

### I. INTRODUCTION

Crystalline silicon-germanium ( $c\text{-Si}_{1-x}\text{Ge}_x$ ) alloys have attracted much attention from both fundamental and technological points of view because they have valuable structural and electronic properties, i.e., a continuous variation in the lattice constants<sup>1,2</sup> and band gaps<sup>2</sup> with changing composition. Although these alloys are known to form solid solutions over the entire composition range, their local structures, such as bond length and coordination, have remained almost unknown.

How atoms form a crystal in a specific structure is a fundamental question in solid-state physics. Two opposite concepts for alloy bond-length dependence on composition have been offered, i.e., Pauling's limit and Vegard's limit. Bragg,<sup>3</sup> and then Pauling and Huggins,<sup>4</sup> noted that the bond lengths in alloys are the sum of their constituent-element atomic radii, and hence should be composition independent (Pauling's limit). Vegard,<sup>5</sup> on the other hand, discovered that the lattice constant  $a(x)$  changes linearly with the composition  $x$ ;  $a(x) = (1-x)a_1 + xa_2$ , where  $a_1$  and  $a_2$  are lattice constants of pure materials, i.e., at  $x=0$  and 1, respectively. On the basis of Vegard's picture, alloys are thought to be sustained by a single bond (Vegard's limit). For example, in a diamond structure, the bond length is given simply as  $\sqrt{3}a(x)/4$ .

In the past ten years, extended x-ray-absorption fine structure (EXAFS) has emerged as a powerful structural tool for the determination of bond lengths between selected atomic pairs. Recent EXAFS experiments on the local structure of ternary semiconductor alloys, such as  $\text{In}_{1-x}\text{Ga}_x\text{As}$  (Refs. 6 and 7) and  $\text{GaAs}_{1-x}\text{P}_x$ ,<sup>8</sup> have led to the conclusion that the bond lengths differ by constitu-

ent atoms, maintaining nearly the respective distances found in pure binary alloys. Theoretical studies, using a valence-force-field theory<sup>9,10</sup> and a pseudopotential perturbation theory,<sup>11</sup> also support distinct bond lengths in alloys. Although a quantitative agreement is not universal in experimental and theoretical studies, it is usually satisfactory to consider the bonding structures of the semiconductor alloys to be closer to Pauling's limit than to Vegard's limit.

Knowledge about the bonding structures of  $c\text{-Si}_{1-x}\text{Ge}_x$  alloys, which are totally covalent, is expected to be a starting point to understand those of largely covalent semiconductor alloys, e.g., GaAs, InAs,  $\text{In}_{1-x}\text{Ga}_x\text{As}$ , etc. Furthermore, in order to clarify the relation between the lattice constant and bonding network, a good understanding of the case of  $c\text{-Si}_{1-x}\text{Ge}_x$  alloys is clearly desirable. EXAFS is a useful probe for studying local structure around atoms of a specific element in alloys. In this paper, by applying EXAFS measurements on  $c\text{-Si}_{1-x}\text{Ge}_x$  with various Ge concentrations, the Ge-Ge and Ge-Si bond lengths, and coordinations on the nearest-neighbor sites around Ge atoms are evaluated.

### II. EXPERIMENTAL PROCEDURES

#### A. Sample preparation

Samples were prepared by rf glow-discharge decomposition of disilane ( $\text{Si}_2\text{H}_6$ ) and germane ( $\text{GeH}_4$ ) mixtures in a capacitively coupled diode system;<sup>12</sup> rf power density was held constant at 0.65 W/cm<sup>2</sup>. Films were grown at a deposition rate of 4.3–13.5 Å/s to a thickness ranging from 0.77 to 2.43 μm on 0.8-mm-thick polycrystalline

graphite substrates. The temperature of the substrate was 300°C, and the pressure was 0.45 Torr during the deposition. Prior to crystallization of amorphous films, hydrogen evolution from as-grown amorphous films was examined when they were heated up to 700°C in a vacuum. Evolution of hydrogen reached the maximum intensity in the temperature range of 300°C–600°C. At 700°C, the evolution intensity became less than 10% of its maximum value. Then it can be assumed that the amount of residual hydrogen is reduced down to a negligible order. Thus, to get crystalline structures, all samples were annealed at 700°C for 5 h in argon atmosphere. Crystallization was confirmed by x-ray diffraction measurements. The dependence of the lattice constant on Ge concentration is shown in Fig. 1. The lattice constant deviates slightly from Vegard's law, shown by the dashed line.

Ge concentration in the film was varied by adjusting the flow rate of Si<sub>2</sub>H<sub>6</sub> and 21% GeH<sub>4</sub> diluted with H<sub>2</sub>, maintaining the total gas-flow rate constant at 20 cm<sup>3</sup> at STP per minute. Chemical composition was determined by inductively coupled argon plasma atomic-emission spectroscopy. Several compositions of Si<sub>1-x</sub>Ge<sub>x</sub> films were prepared with different Ge concentrations;  $x=0.20, 0.39, 0.61, 0.82, \text{ and } 1.0$ .

### B. Measurements

The EXAFS measurements were carried out at the EXAFS station (Beam line 8C) (Ref. 13) of the Photon Factory at the National Laboratory for High Energy Physics in Tsukuba, Japan. The electron storage ring was operated at 2.5 GeV; the beam current ranged from 140 to 260 mA during the measurements.

The x-ray absorption spectra were taken on the *K* edge of Ge, using a monochromator equipped with a Si(111) double crystal. The monochromator was detuned so as to eliminate the influence of high-order harmonics. The intensity of higher-order harmonics was checked as being less than 1% with a NaI scintillation counter. The ab-

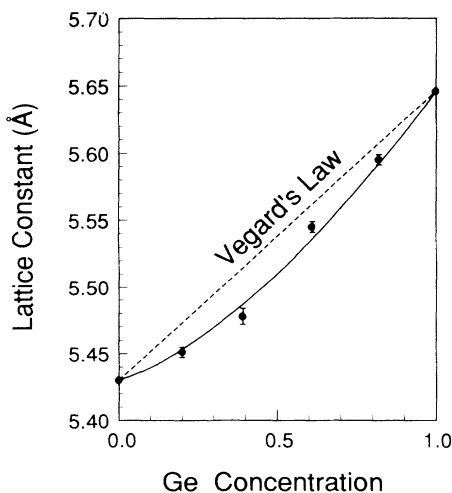


FIG. 1. Change in lattice constant with Ge concentration  $x$  in crystalline Si<sub>1-x</sub>Ge<sub>x</sub> alloys, determined by x-ray-diffraction measurement. The dashed line represents Vegard's law.

sorption measurements were performed in the transmission mode at room temperature. The incident and transmitted x-ray intensities  $I_0$  and  $I$ , respectively, were monitored simultaneously with two ionization chambers. Here,  $\ln(I_0/I)$  is equal to  $\mu t$ , where  $\mu$  is the linear absorption coefficient and  $t$  is the absorber thickness. To get the optimum absorption coefficient jump ( $\mu t \approx 1$ ) at the absorption edge, several sheets of the same type film were stacked. The measured energy range was from 500 eV below to 1000 eV above the absorption edge. The energy resolution was estimated to be 1–2 eV.

### C. Analysis

Photoelectrons ejected from an x-ray-absorbing atom can be characterized by photoelectron wave number  $k$ ;

$$k = \left[ \frac{2m}{\hbar^2} (h\nu - E_0) \right]^{1/2}, \quad (1)$$

where  $m$  is the electron mass,  $h\nu$  is the incident photo energy, and  $E_0$  is the absorption-edge energy. The normalized EXAFS oscillation  $\chi(k)$  is defined as a function of  $k$ , i.e.,

$$\chi(k) = [\mu(k) - \mu_0(k)] / \mu_0(k), \quad (2)$$

where  $\mu(k)$  and  $\mu_0(k)$  are the *K*-shell absorption coefficient for atoms in environment and for isolated atoms, respectively. Both  $\mu(k)$  and  $\mu_0(k)$  are obtained in the conventional manner.<sup>14</sup>  $\chi(k)$  is multiplied by  $k^3$  to intensify higher  $k$  contributions. Experimental EXAFS,  $k^3\chi(k)$ , is analyzed using the formula based on a spherical-wave approximation on the emitted photoelectrons.<sup>15–17</sup> Fitting parameters are also follows: Ge-Ge and Ge-Si bond lengths; Ge coordination ratio defined by  $N_{\text{Ge}}/4$ , where  $N_{\text{Ge}}$  is the average number of nearest Ge atoms around Ge atoms and 4 is the number of nearest neighbors in the perfect diamond structure of pure Ge crystal; deviation of Debye-Waller factors of Ge and Si atoms from the pure crystal values. The physical quantities needed for calculation were obtained as follows. Phase shifts of the photoelectron in the absorbing atom are taken from numerical tables given by Teo and Lee<sup>18</sup> with Herman-Skillman wave functions.<sup>19</sup> Phase shifts for the scattering atom ( $l=0-12$ ) were calculated by a program developed by Pendry<sup>20</sup> with core-state wave functions.<sup>18</sup> The effect of thermal vibration of scattering atoms in pure Ge and Si crystals is included in the thermal Debye parameter.<sup>21</sup> The photoelectron inelastic scattering effect can be presented in the form  $\exp(-2r/\lambda)$ , where  $r$  is the interatomic path length and  $\lambda$  is the mean free path. For the mean free path, the escape depth dependence on photoelectron energy of crystalline germanium, measured by Gant and Mönch,<sup>22</sup> is used.

## III. RESULTS

The Ge *K*-edge absorption spectra for Ge concentrations of (a) 1.0, (b) 0.61, and (c) 0.20 are shown in Fig. 2; background absorption is subtracted in each spectrum.

The absorption-edge energy  $E_0$  is a fundamental quantity which controls a reliability of analysis.<sup>23</sup> In the present study, the  $E_0$  value for the  $K$  edge of Ge was determined as the steepest point of the edge jump on the experimental absorption spectrum: 11 090.0 eV for  $x=1.0$  and 11 087.0 eV for  $x=0.20$ –0.82.

The experimental  $k^3\chi(k)$ , obtained with the above  $E_0$  values, is Fourier-transformed into  $r$  space as follows:

$$F(r) = \sqrt{2/\pi} \int_{k_{\min}}^{k_{\max}} k^3 \chi(k) W(k) e^{-2ikr} dk, \quad (3)$$

where  $k_{\min}$  and  $k_{\max}$  are lower and upper limits of the Fourier transform, respectively, and  $W(k)$  is a window function to reduce the cutoff effect, given by

$$W(k) = \begin{cases} 1.0 - \cos\left[\frac{\pi}{2}(k - k_{\min})/\Delta k\right] & \text{for } k_{\min} < k < k_{\min} + \Delta k, \\ 1.0 & \text{for } k_{\min} + \Delta k < k < k_{\max} - \Delta k, \\ 1.0 - \cos\left[\frac{\pi}{2}(k - k_{\max})/\Delta k\right] & \text{for } k_{\max} - \Delta k < k < k_{\max}. \end{cases} \quad (4)$$

In the present analysis,  $k_{\min}$  and  $k_{\max}$  are 3.0 and 14.0  $\text{\AA}^{-1}$ , respectively, and  $\Delta k$  is 0.1  $\text{\AA}^{-1}$ . Absolute values of  $F(r)$  for  $x=1.0$ , 0.61, and 0.20 are shown in Fig. 3. The peak intensity is reduced and the distance is shortened by decreasing Ge content. Main peaks near  $r=2$   $\text{\AA}$  are due to the nearest-neighbor atoms around Ge atoms. In order to clarify the bonding structures, the main peaks are Fourier-transformed back into  $k$  space in the same manner as described above. In Fig. 4, solid lines

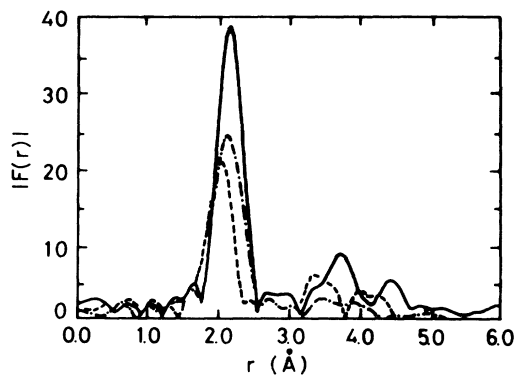


FIG. 3. Absolute values of Fourier transform of  $k^3\chi(k)$  into  $r$  space,  $|F(r)|$ , corresponding to  $x=1.0$  (solid line),  $x=0.62$  (dashed-dotted line), and  $x=0.20$  (dashed line). The Fourier transform range employed was from 3.0 to 14.0  $\text{\AA}^{-1}$  for each sample. Main peaks near  $r=2.0$   $\text{\AA}$ , which are nearest-neighbor contributions, were Fourier-transformed back into  $k$  space for the fitting procedure.

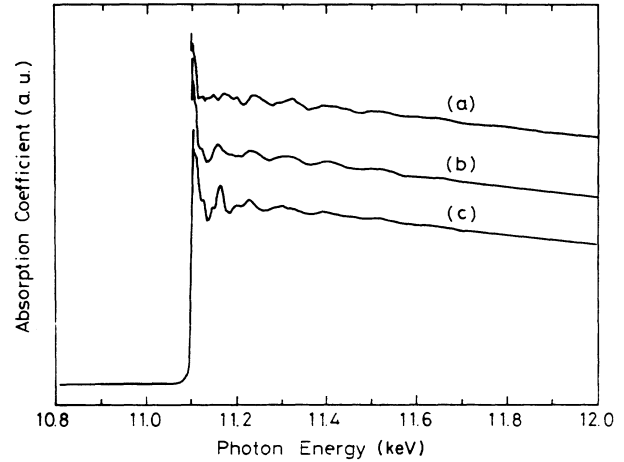


FIG. 2. Experimental x-ray absorption vs photon energy curves for crystalline  $\text{Si}_{1-x}\text{Ge}_x$  alloys at room temperature: (a)  $x=1.0$ , (b)  $x=0.61$ , and (c)  $x=0.20$ .

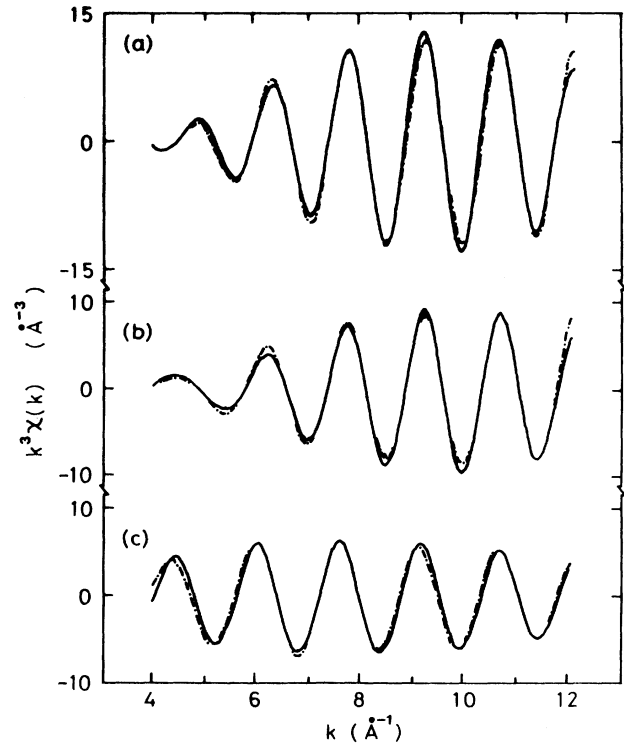


FIG. 4. Experimental  $k^3\chi(k)$ , due to nearest-neighbor atoms around a Ge atom, is shown by the solid line for (a)  $x=1.0$ , (b) 0.61, and (c)  $x=0.20$  in crystalline  $\text{Si}_{1-x}\text{Ge}_x$  alloys. Dashed-dotted lines in (a), (b), and (c) represent the best-fit results.

TABLE I. Determined structure parameters in the fitting procedure, and reliability factors ( $R$  factor). Column 1: Ge concentration  $x$  in crystalline  $\text{Si}_{1-x}\text{Ge}_x$ , determined by inductively coupled plasma spectroscopy. Column 2: Ge coordination ratio  $X_c$ , defined by  $N_{\text{Ge}}/4$ , where  $N_{\text{Ge}}$  is the number of nearest-neighbor Ge atoms around a Ge atom and 4 is the number of nearest-neighbor atoms in perfect diamond structure. Columns 3 and 5: Ge-Ge and Ge-Si bond length, respectively. Columns 4 and 6: deviation of Debye-Waller factors for Ge and Si atoms from that of pure Ge and Si crystals, respectively. Column 7:  $R$  factor of best-fit results.

$x$	$X_c$	$R_{\text{Ge-Ge}}$ ( $\text{\AA}$ )	$(\Delta\sigma)_{\text{Ge}}^2$ ( $\text{\AA}^2$ )	$R_{\text{Ge-Si}}$ ( $\text{\AA}$ )	$(\Delta\sigma)_{\text{Si}}^2$ ( $\text{\AA}^2$ )	$R$ factor
1.00		2.446	$6.0 \times 10^{-6}$			0.217
0.82	0.84	2.446	$5.2 \times 10^{-4}$	2.398	$6.3 \times 10^{-4}$	0.175
0.61	0.67	2.444	$3.4 \times 10^{-4}$	2.396	$7.8 \times 10^{-4}$	0.165
0.39	0.39	2.443	$4.2 \times 10^{-4}$	2.397	$1.0 \times 10^{-9}$	0.140
0.20	0.17	2.445	$4.8 \times 10^{-12}$	2.395	$1.5 \times 10^{-9}$	0.129

represent experimental  $k^3\chi(k)$  due to the nearest-neighbor atoms, for (a)  $x=1.0$ , (b) 0.61, and (c) 0.20. Best-fit results, summarized in Table I, are shown by dashed-dotted lines. Excellent agreement exists between the experimental and the theoretical curves.

Figure 5 shows the coordination ratio as a function of the Ge concentration. The Ge coordination ratio is a criterion for the extent of atomic mixing. If a site-occupation probability is proportional to the alloy composition, in other words, atoms are distributed randomly and the Ge coordination ratio is identical to the Ge concentration. EXAFS analysis shows that the Ge coordination ratio is almost equal to the Ge concentration, which means a random mixing of Si and Ge atoms is essential in  $c\text{-Si}_{1-x}\text{Ge}_x$  alloys with the Ge concentrations ranging from 0.20 to 0.82.

Figure 6 shows the Ge-Ge bond length  $R_{\text{Ge-Ge}}$  and the Ge-Si bond length  $R_{\text{Ge-Si}}$  in  $c\text{-Si}_{1-x}\text{Ge}_x$  alloys as a function of the Ge concentration. It is noteworthy that the bonds tend to maintain their respective lengths over the composition range studied: nearly 2.45  $\text{\AA}$  for the Ge-Ge bond and 2.40  $\text{\AA}$  for the Ge-Si bond. The bond lengths are almost identical to the sum of their atomic radii (1.22 and 1.17  $\text{\AA}$  for Ge and Si, respectively), as noted by Pauling *et al.* The Si-Si bond length in the alloys has not been investigated in this study. It is expected, by analogy to the Ge-Ge and Ge-Si cases, that the Si-Si bond length is close to 2.35  $\text{\AA}$ , which is the sum of the Si atomic ra-

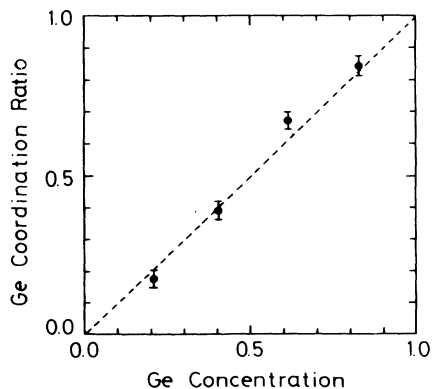


FIG. 5. Ge coordination ratio around Ge atoms,  $N_{\text{Ge}}/4$ , as a function of Ge concentration  $x$  in crystalline  $\text{Si}_{1-x}\text{Ge}_x$  alloys. The dashed line shows the Ge coordination ratio expected for a random mixture of Si and Ge atoms.

dius. In our previous papers,<sup>23,24</sup> the local structures of amorphous  $\text{Si}_{1-x}\text{Ge}_x\text{:H}$  alloys have been studied. It was concluded that the Ge-Ge and Ge-Si bond lengths are 2.46 and 2.41  $\text{\AA}$ , respectively. The Ge-Ge and Ge-Si bond lengths are almost the same in the amorphous and crystalline alloys.

#### IV. DISCUSSION

In the present analysis, deviations from thermal Debye parameters  $B_{293\text{K}}$  for pure Ge and Si crystals at room temperature, are also evaluated. It should be noted here that the deviations are negligible, being less than  $7.8 \times 10^{-4} \text{\AA}^2$  for the Ge concentrations studied, compared to the  $B_{293\text{K}}$  values for Ge and Si crystals, 0.31 and 0.30 s, respectively. Negligible deviation means that Debye-Waller factors are equal to those in pure Ge and Si crystals. Therefore, phonon anomaly associated with alloying does not exist in polycrystalline  $\text{Si}_{1-x}\text{Ge}_x$  systems. In amorphous  $\text{Si}_{1-x}\text{Ge}_x\text{:H}$  alloys, EXAFS measure-

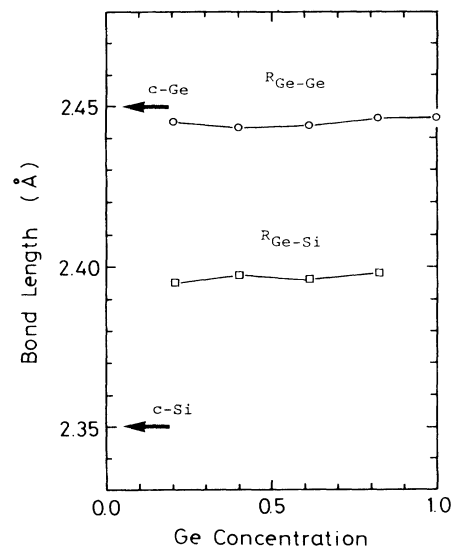


FIG. 6. Ge-Ge bond length  $R_{\text{Ge-Ge}}$  (open circles) and Ge-Si bond length  $R_{\text{Ge-Si}}$  (open squares), as a function of Ge concentration  $x$  in crystalline  $\text{Si}_{1-x}\text{Ge}_x$  alloys. Bond lengths are concentration independent and nearly equal to  $R_{\text{Ge-Ge}}=2.45 \text{\AA}$  and  $R_{\text{Ge-Si}}=2.40 \text{\AA}$ , respectively. The bond lengths in Ge crystals ( $c\text{-Ge}$ ) and Si crystals ( $c\text{-Si}$ ) are indicated by arrows.

ments<sup>25</sup> have shown that Debye-Waller factors are the same for Ge-Ge and Ge-Si bonds over Ge concentrations from 0.20 to 0.89, and that they are similar to the amorphous Ge:H case. The Debye-Waller factor is the sum of thermal and static contributions. Minomura *et al.*<sup>26</sup> indicated, from Raman measurements, that static contributions are the same for Ge-Ge and Ge-Si bonds in amorphous  $\text{Si}_{1-x}\text{Ge}_x$  alloys. They concluded that static contribution to the Debye-Waller factors is constant in amorphous  $\text{Si}_{1-x}\text{Ge}_x$  alloys. The lack of Raman measurements in this paper prevents us from distinguishing thermal and static contributions.

If bonds contract and/or stretch, the Debye-Waller factors should be affected through the force constant, as a consequence of distortion of electronic configurations. No evidence in Debye-Waller factor anomaly in  $c\text{-Si}_{1-x}\text{Ge}_x$  alloys is seen to support the above hypothesis. Hence, the Debye-Waller factor behavior reinforces the constant bond lengths, as shown in Fig. 6.

Martin and Zunger<sup>9</sup> have investigated systematic lattice distortions around isovalent impurities, using a valence-force-field theory.<sup>27,28</sup> They defined the dimensionless relaxation parameter in ternary ( $A_{1-x}B_xC$ ) alloys as

$$\xi = [R_{BC}(AC:B) - R_{AC}] / (R_{BC} - R_{AC}), \quad (5)$$

where  $R_{AC}$  and  $R_{BC}$  are bond lengths in two pure binary materials, respectively, and  $R_{BC}(AC:B)$  is the  $BC$  bond length around the  $B$  impurities in the  $AC$  host crystal. It has been predicted that  $\xi$  is in the range of 0.6–0.8 for most semiconductors, closer to Pauling's limit rather than to Vegard's limit. On the other hand, Ito<sup>11</sup> has estimated the  $\xi$  value for ternary semiconductor alloys, using a pseudopotential perturbation theory.<sup>29</sup> Calculated results are in the range of 0.2–0.3 for most  $A_{1-x}B_xC$  alloys.

EXAFS results on ternary semiconductor alloys seem to support Pauling's picture. In  $\text{Ga}_{1-x}\text{In}_x\text{As}$  alloys,<sup>6,7</sup> it has been shown that the Ga-As and In-As nearest-neighbor distances remain nearly constant, varying by only 0.04 Å:  $\xi=0.77$  for  $\text{Ga}_{1-x}\text{In}_x\text{As}$ . In  $\text{GaAs}_{1-x}\text{P}_x$  systems,<sup>8</sup> the Ga-As and Ga-P nearest-neighbor distances differ from each other, showing slight variations with composition:  $\xi=0.60$  for  $\text{GaAs}_{1-x}\text{P}_x$ . In the present  $c\text{-Si}_{1-x}\text{Ge}_x$  case,  $\xi$  is close to 1.0, indicating that Pauling's picture is valid in covalent binary alloys. It should be noted that previous results on ternary systems were obtained using a conventional curve-fitting analysis, which is based on plane waves of emitted photoelectrons.<sup>30</sup> In general, it is possible to reliably estimate bond lengths in alloys if model compounds whose local structures are well known are available.<sup>31</sup> Thus it is relatively hard to say positively, for complex systems, whether bond length varies slightly with composition or not. Whether or not it does in covalent and largely covalent semiconductors, we may conclude that the constituent bonding elements determine bond lengths, according to Pauling's picture. In contrast to the case of semiconductor alloys, a larger relative change in bond length has been reported on ionic  $\text{K}_{1-x}\text{Rb}_x\text{Br}$  (Ref. 32) alloys, indi-

cating that bonding structures differ in ionic and covalent alloys.

Ichimura *et al.*<sup>10</sup> have recently calculated the bond lengths in crystalline  $\text{Si}_{1-x}\text{Ge}_x$  alloys by a valence-force-field (VFF) model. The  $\xi$  values for Ge-Ge, Si-Si, and Ge-Si bonds are about 0.6, which is consistent with the result obtained by Martin and Zunger.<sup>9</sup> However, a serious discrepancy exists between the VFF calculation and the present EXAFS analysis. Two possible reasons are presented here. One is an overestimation of force constants in the VFF calculation. It is not certain that the microscopic lattice relaxation can be successfully described by the force constant which is itself derived from a macroscopic force constant. The other possibility is that exclusion of anharmonicity in the VFF model might have a non-negligible effect on results. In either case, the reason for the discrepancy requires further study.

The bond angle must be modified to form a unit cell with a bond of a distinct length. According to the Pauli exclusion principle, covalently bonded atoms interact with a strong repulsive force. Considering that the diamond structure gives a low filling of space, 0.34 of the available space, it is advantageous to maintain bond length. Therefore, the structural change occurs more often in bond angles than in bond lengths. As shown in Fig. 5, atoms are randomly mixed in the alloys. Accordingly, in triangle configurations of  $\text{Si-Ge-Si}$ ,  $\text{Ge-Ge-Ge}$ , and  $\text{Ge-Ge-Si}$  (underlines represent central atoms), bond angles must also be distinctly fixed for each configuration. Thus, if the bond angle distribution could be measured, the shape of the distribution profile would be dependent on the Ge concentration.

As already shown in Fig. 1, the lattice constant changes with composition, deviating slightly from Vegard's law. Since the lattice constant is an average over many unit cells, it does not deliver detailed information about nearest-neighbor atoms. One can expect that the degree of bond-angle distortion would approach its maximum value in the midpoint composition, provided that bond lengths between randomly mixed atoms do not vary with composition. The bonding-network model, which can explain clearly both lattice constant behavior and bond length, is now required. For that purpose, next-nearest-neighbor structure should be also clarified. At present, a nonlinear variation in a lattice constant may be regarded as a consequence of the invariant bond lengths.

## V. CONCLUSION

The local structures of  $c\text{-Si}_{1-x}\text{Ge}_x$  alloys have been determined using the EXAFS method. It is shown that Ge-Ge and Ge-Si bonds relax completely, while the lattice constant varies monotonically. Significant changes in the bond lengths versus Ge concentration ranging from 0.20 to 0.82 are not detected; nearly 2.45 Å for Ge-Ge bonds and 2.40 Å for Ge-Si bonds. A study of the coordination around Ge atoms has shown that atoms are randomly mixed within the Ge concentration range studied. These results support the Bragg and Pauling notion that bond lengths in alloys are the sum of their constituent-

element atomic radii and that they are independent of composition.

#### ACKNOWLEDGMENTS

The authors are grateful to Dr. Masaya Ichimura of Nagoya Institute of Technology for valuable discussion and comments regarding atomic-scale structures of semiconductor alloys. They also acknowledge Tsutomu Ishi-

ba for x-ray measurements. We are deeply indebted to Dr. Akira Fukuhara of Advanced Research Laboratory of Hitachi, Ltd. and to Dr. Masaharu Nomura of National Laboratory for High Energy Physics, for guiding EXAFS calculation. This study was performed with the approval of the Photon Factory Advisory Council, Proposal No. 87-0012. This work was supported by the New Energy Technology Development Organization as a part of the Sun Shine Project under the Ministry of International Trade and Industry.

- <sup>1</sup>J. P. Dismukes, L. Ekstrom, and R. J. Paff, *J. Phys. Chem.* **68**, 3021 (1964).
- <sup>2</sup>E. R. Johnson and S. M. Christian, *Phys. Rev.* **95**, 560 (1954).
- <sup>3</sup>W. L. Bragg, *Philos. Mag.* **40**, 169 (1920).
- <sup>4</sup>L. Pauling and M. L. Huggins, *Z. Kristallogr. Kristallgeom. Kristallphys. Kristallchem.* **87**, 205 (1934).
- <sup>5</sup>L. Vegard, *Z. Phys.* **5**, 17 (1921).
- <sup>6</sup>J. C. Mikkelsen, Jr. and J. B. Boyce, *Phys. Rev. Lett.* **49**, 1412 (1982).
- <sup>7</sup>J. C. Mikkelsen, Jr. and J. B. Boyce, *Phys. Rev. B* **28**, 7130 (1983).
- <sup>8</sup>T. Sasaki, T. Onda, R. Ito, and N. Ogasawara, *Jpn. J. Appl. Phys.* **25**, 231 (1986).
- <sup>9</sup>L. Martin and A. Zunger, *Phys. Rev. B* **30**, 6217 (1984).
- <sup>10</sup>M. Ichimura, Y. Nishino, H. Kajiyama, and Takao Wada, *Jpn. J. Appl. Phys.* **29**, 842 (1990).
- <sup>11</sup>T. Ito, *Jpn. J. Appl. Phys.* **26**, 256 (1987).
- <sup>12</sup>S. Muramatsu, S. Kokunai, Y. Nishino, H. Kajiyama, S. Matsubara, H. Itoh, N. Nakamura, and T. Shimada, *Appl. Surf. Sci.* **33-34**, 735 (1987).
- <sup>13</sup>Y. Suzuki, H. Sekiyama, Y. Hirai, K. Hayakawa, H. Kajiyama, T. Hirano, K. Usami, and T. Takagi, *Jpn. J. Appl. Phys.* **27**, L149 (1988).
- <sup>14</sup>M. Nomura, K. Asakura, U. Kaminaga, T. Matsusita, K. Kohra, and H. Kuroda, *Bull. Chem. Soc. Jpn.* **55**, 3911 (1982).
- <sup>15</sup>A. Fukuhara and H. Kajiyama (unpublished).
- <sup>16</sup>A. G. Mckale, B. W. Veal, A. P. Paulikas, S.-K. Chan, and G. S. Knapp, *J. Am. Chem. Soc.* **110**, 3763 (1988).
- <sup>17</sup>J. E. Muller and W. L. Schaich, *Phys. Rev. B* **27**, 6489 (1983).
- <sup>18</sup>B.-K. Teo and P. A. Lee, *J. Am. Chem. Soc.* **101**, 2815 (1979).
- <sup>19</sup>F. Herman and S. Skillman, *Atomic Structure Calculations* (Prentice-Hall, Englewood Cliffs, NJ, 1963).
- <sup>20</sup>J. B. Pendry, *J. Phys. C* **4**, 2501 (1971); **5**, 2567 (1972); the program is listed by J. B. Pendry, *Low-Energy Electron Diffraction* (Academic, New York, 1974).
- <sup>21</sup>*International Tables for X-ray Crystallography, Vol. III*, edited by K. Lonsdale *et al.* (Kynoch, Birmingham, 1962).
- <sup>22</sup>H. Gant and W. Mönch, *Surf. Sci.* **105**, 217 (1981).
- <sup>23</sup>H. Kajiyama, A. Fukuhara, Y. Nishino, and S. Muramatsu, *Phys. Rev. B* **38**, 1938 (1988).
- <sup>24</sup>Y. Nishino, S. Muramatsu, Y. Takano, and H. Kajiyama, *Phys. Rev. B* **38**, 1942 (1988).
- <sup>25</sup>L. Incoccia, S. Mobilio, M. G. Proietti, P. Fiorini, C. Giovannella, and F. Evangelisti, *Phys. Rev. B* **31**, 1028 (1985).
- <sup>26</sup>S. Minomura, K. Tsuji, M. Wakagi, T. Ishidate, K. Inoue, and M. Shibuya, *J. Non-Cryst. Solids*, **59-60**, 541 (1983).
- <sup>27</sup>P. N. Keating, *Phys. Rev.* **145**, 637 (1966).
- <sup>28</sup>C. V. Fong, W. Weber, and J. C. Phillips, *Phys. Rev. B* **12**, 5387 (1976).
- <sup>29</sup>W. A. Harrison, *Pseudopotential in the Theory of Metals* (Benjamin, New York, 1966).
- <sup>30</sup>P. A. Lee and J. B. Pendry, *Phys. Rev. B* **11**, 2795 (1975).
- <sup>31</sup>B.-K. Teo, M. A. Antonio, and B. A. Aveill, *J. Am. Chem. Soc.* **105**, 3751 (1983).
- <sup>32</sup>J. B. Boyce and J. C. Mikkelsen, Jr., in *EXAFS and Near Edge Structure*, edited by K. O. Hodgson, B. Hedman, and J. E. Penner-Hahn, *Proceedings in Physics Vol. 2* (Springer, Berlin, 1984), p. 426.